Landau-Zener Transitions in Frozen Pairs of Rydberg Atoms

Nicolas Saquet, Anne Cournol, Jérôme Beugnon,* Jacques Robert, Pierre Pillet, and Nicolas Vanhaecke†

Laboratoire Aimé Cotton, CNRS, Bâtiment 505, Université Paris-Sud, 91405 Orsay, France

(Received 18 September 2009; published 2 April 2010)

We have induced adiabatic transitions in pairs of frozen Rydberg sodium atoms of a supersonic beam. The diatomic $ns + ns \rightarrow np + (n-1)p$ transition takes place in a time-dependent electric field and originates from the adiabatic change of the internal state of the pair induced by the dipole-dipole interaction. This is experimentally achieved by sweeping an electric field across the energy degeneracy $ns\,ns - np(n-1)p$. Our results fully agree with a two-level Landau-Zener model in the diatom system.

DOI: 10.1103/PhysRevLett.104.133003 PACS numbers: 32.80.Ee, 32.60.+i, 37.20.+j

Samples of Rydberg atoms have long been known to exhibit enormous long-range interactions and to be particularly suited for observation thanks to their very long radiative lifetimes. This has stimulated a variety of investigations aiming at controlling these long-range interactions. Dipole-dipole interactions between Rydberg atoms [1] have been investigated first through thermal energy collisions [2], and radiatively assisted collisions [3], then through energy transfers in frozen Rydberg gases [4–6], in which the relative motion of the atoms becomes negligible on the time scale of the experiment. Fascinating prospects in quantum information science have triggered many experiments on the Rydberg excitation blockade in cold atomic ensembles, a key ingredient for quantum gates [7,8]. The dipole blockade, induced by dipole-dipole interactions, has been observed at Förster resonances [9]. These blockade effects have led to the observation of collective Rydberg excitation, which produces a highly entangled many-body state [10–12].

In this Letter, we report on the control of the internal state of pairs of Rydberg atoms in a supersonic beam, which constitutes a step forward toward correlations within pairs, and toward the entanglement within such pairs. Such an entanglement opens the possibility to investigate Rydberg pair interferences in a supersonic beam and constitutes a pathway of fine-tuning of reactive scattering. It is also of great importance in the context of dipole blockade and controlled interactions between Rydberg atoms, especially in the quest of neutral-atom quantum gates using two or more interacting atoms [11,12].

When pairs of Rydberg atoms experience a time-varying electric field, the adiabatic following of states depends parametrically on the interatomic distance (see Fig. 1, top right), as the Rydberg atoms interact via the dipole-dipole interaction, which scales as r^{-3}, where r stands for the interatomic distance. In the present work, thanks to a time-varying applied electric field, a given pair of Rydberg atoms experiences two passages back and forth across an avoided crossing induced by the dipole-dipole interaction. We identify pairs of Rydberg atoms which have experienced exactly one adiabatic and one diabatic transition. This is allowed by the temperature (≃1 K) of our supersonic atomic beam: the motion within a pair of atoms is frozen on the time scale of a single passage, but the interatomic distance evolves significantly between the two passages, as represented by the trajectory on Fig. 1 (top right). Starting from $ns + ns$ Rydberg atom pairs (initial pair state) and by ramping the electric field back and forth across the avoided crossing, pairs of $np + (n-1)p$ atoms are produced (final pair state). Our results fully agree with a model based on Landau-Zener (LZ) passages, which are responsible for the multiple paths in the pulsed-field ionization (PFI) of both diluted gases and dense frozen gases of Rydberg atoms [13,14]. In the PFI of dense Rydberg gases, the many-body avoided crossings can be traversed adiabatically, resulting in an apparent modification of the threshold ionization field [14].

The experimental setup consists of an atomic beam machine, schematically depicted in Fig. 1. A pulsed supersonic beam of ground-state sodium atoms is produced by

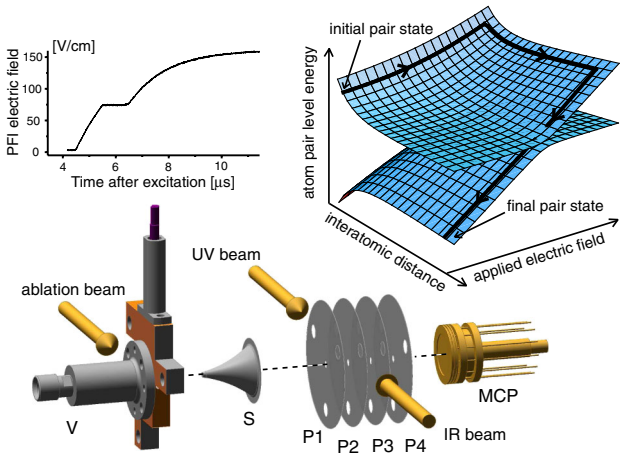

FIG. 1 (color online). Top right: Atom pair level energies as a function of interatomic distance and electric field, as well as a schematic path followed by a given pair as time goes by. Top left: Measured time dependence of the PFI electric field, starting 4.5 μs after the optical excitation of the atoms (see text). Bottom: Experimental setup.

expanding helium through a solenoid valve (V) (General Valve series 9, repetition rate 10 Hz, stagnation pressure 6 bars) in vacuum, using the technique of laser-induced ablation of sodium. On the front plate of the valve is mounted an ablation chamber, in which a rotating rod of solid sodium is ablated by focusing on it the output of a frequency-doubled pulsed YAG laser (Ekspla 220NL, 1.1 mJ/pulse at 532 nm). The beam passes through a skimmer (S) (Molecular Beams, 0.8 mm diameter) 20 mm downstream from the exit of the ablation chamber and enters the experimental chamber. This chamber hosts four cylindrical copper plates ($P1 - P4$), 10.0 mm apart from each other, with a 3 mm-diameter opening in their center, through which the atoms fly. The supersonic atomic beam has a mean velocity of about 1900 m/s and a temperature on the order of 1 K. We excite the sodium atoms into a well-controlled Rydberg state using a two-color resonant excitation $3S_{1/2} \rightarrow 4P_{3/2} \rightarrow ns$. Between $P2$ and $P3$, the atomic beam intersects counterpropagating ultraviolet (UV) and infrared (IR) laser beams (both $\simeq$2 mm waist) at right angles. The UV radiation is tuned to the $3S_{1/2} - 4P_{3/2}$ transition and is produced by a frequency-doubled pulsed dye laser (Continuum ND6000, 7 ns pulse, 150 μJ/pulse at 330 nm, 1.5 GHz bandwidth). The IR radiation is provided by a cw Ti:sapphire laser (Coherent MBR110, up to 1.5 W at 910 nm) and is tuned to resonance with the desired ns Rydberg state. From laser-induced fluorescence measurements carried out on our beam of sodium atoms in the ground state, we evaluate the density of Rydberg atoms to be about 1×10^8 cm^{-3}. Plates $P2$ and $P3$ are used to apply a (time-dependent) electric field to the Rydberg atoms after the excitation. Plates $P3$ and $P4$ are used to pulsed-field ionize the Rydberg states. The subsequent ions are then accelerated toward microchannel plates (MCP) located 8 cm downstream from $P4$.

The top left panel of Fig. 1 shows a typical electric field used for pulsed-field ionization, which is obtained by applying exponentially rising voltages on $P3$ and $P4$. These voltages are set to ionize atoms in the np state just below the field of the plateau, while atoms in the ns or $(n-1)p$ state are ionized in the second rising part of the electric field. This allows us to fully separate the time-of-flight profiles of the ions originating from the np states and from the ns and $(n-1)p$ states. Both signals are then gated and integrated for acquisition and treatment.

The optical excitation of the atoms into the ns Rydberg state is done under field-free conditions, then a variable homogeneous electric field is applied for 1.2 μs between $P2$ and $P3$, starting 600 ns after the excitation (see Fig. 2, right panel). The cloud of Rydberg atoms flies slowly enough such that the atoms experience both the rising and the falling of the electric field, which vary exponentially with a time constant of 220 ns. We denote hereafter F_n the value of the electric field which induces the energy degeneracy of the Rydberg atom pair in the states $ns + ns$ and $np + (n-1)p$ (see Fig. 2, left panel).

On Fig. 3 are reported the normalized ion signals resulting from the np state, as a function of the applied electric field, while the optical excitation is done into the ns state [curve (a): $n = 53$, (b): $n = 48$, (c): $n = 43$]. The signals have been normalized to the total ion signal resulting from the pulsed-field ionized Rydberg states. Each data point results from a 1000-shot measurement and the indicated error bars are inferred from ten such measurements. As a function of the applied electric field, three behaviors are clearly identified. If the applied field F lies below F_n, a small background signal of np states is present. It results from the blackbody radiation absorption by atoms in the ns state and is not different than in zero field in this range of electric field strength [15]. For the sake of clarity, we have set the origin of the vertical axis of all figures to this blackbody-induced background signal. If the applied field is equal to F_n, an additional production of np states is observed, due to resonant collisions between ns atoms taking place at this field. Although not resolved in our experiment, four collision resonances take place in the vicinity of this field, due to the fine structure of the np and $(n-1)p$ states [2]. If the applied field lies above the resonance field F_n, then the atoms experience a time-varying electric field which crosses the field of the $ns\,ns - np(n-1)p$ energy degeneracy. In this case, independently of the amplitude of the applied field, we observe the appearance of a significant amount of additional atoms in the np state.

In order to explain these results, let us consider the time dependence of the electric field F, which crosses the field F_n. Within a pair of Rydberg atoms at a distance r from each other, the dipole-dipole interaction, which scales as r^{-3}, removes the energy degeneracy and the energy curves exhibit an avoided crossing (left panel of Fig. 2). Using a

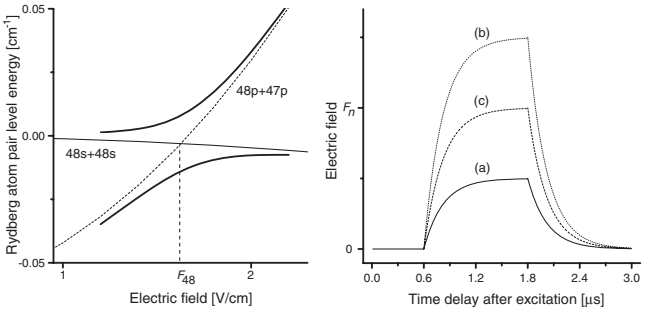

FIG. 2. The left panel shows the level energies of a pair of Rydberg sodium atoms, showing the $48s + 48s - 48p + 47p$ energy degeneracy, which occurs at the electric field F_{48}. A schematic removal of the energy degeneracy by the dipole-dipole interaction is also represented (bold line). The right panel schematically shows the time dependence of the applied electric field F, for three values of its strength. (a) $F < F_n$, (b) $F > F_n$, (c) $F \simeq F_n$.

LZ picture, we evaluate the probability that a pair of Rydberg atoms initially prepared in the ns state undergoes an adiabatic transition across the avoided crossing [16,17]. This reads

$$P_{\mathrm{ad}} = 1 - \exp[-(r/r_0)^{-6}], \quad (1)$$

with

$$r_0 = \left(\frac{2\pi|\langle ns|\mu|np\rangle|^2|\langle ns|\mu|(n-1)p\rangle|^2}{(4\pi\epsilon_0)^2\hbar\Delta\mu(dF/dt)}\right)^{1/6}, \quad (2)$$

where $\langle ns|\mu|np\rangle$ [respectively $\langle ns|\mu|(n-1)p\rangle$] is the electric dipole matrix element connecting the ns and the np [respectivel $(n-1)p$] states, $\Delta\mu$ stands for the difference in effective dipole moment between pair states $ns + ns$ and $np + (n-1)p$, while dF/dt is the rate at which the electric field changes in time, taken at the field of the avoided crossing F_n. Given the time-dependent electric field used in our experiment, rising in 220 ns, and for atoms initially prepared in the $48s$ state, one finds $r_0 \simeq 5\ \mu$m. The probability P_{ad} for an adiabatic transition of the Rydberg pair exhibits a sharp behavior as a function of r, effectively converting all pairs of ns atoms with an interatomic distance smaller than r_0 into pairs in the $np + (n-1)p$ state. At our atomic beam density, the fraction of Rydberg atoms having their nearest neighbor at less than r_0 is calculated to be about 5%. This implies a transfer of atoms from the initial $48s$ state to one of the $48p$ or $47p$ of 5%, hence a production of atoms in the $48p$ state through an adiabatic LZ transition of 2.5% of the initial $48s$ Rydberg atoms.

Let us emphasize here three points which back up the presented model. (i) This model assumes that the pairs of Rydberg atoms are frozen during the time the avoided crossing is traversed. We can define a typical duration of the crossing [16,17], which shows that the relative motion of a pair of Rydberg atoms during the crossing is about 100 nm, much smaller than the interatomic distance r_0 evaluated previously. (ii) As mentioned above, because of the fine structure of the p states, the Stark map of the atom pair exhibits actually four avoided crossings. Two adjacent avoided crossings are separated by about 100 mV/cm in terms of electric field in the case of $n = 48$. Given the rising time of the applied electric field and the temperature of the Rydberg cloud, this corresponds to a typical relative motion in a pair of atoms of about 500 nm. Therefore, to a good approximation, only the first resonance that is crossed plays a role. (iii) In the experiment described above, the electric field is first ramped up, then down, crossing twice the field F_n 1.2 μs apart in time (see Fig. 2, right panel). During this 1.2 μs, the atoms of a given pair move relative to each other by more than 20 μm. Therefore, a pair of atoms which experiences an adiabatic transition at the rise of the electric field will very likely undergo a diabatic transition at the fall of the electric field 1.2 μs later (path represented by the thin line in the inset of Fig. 3, see also Fig. 1 top right). When the avoided crossing is traversed for the second time, however, other pairs of ns atoms fulfill the condition for an adiabatic transition, which had experienced a diabatic transition at the rise of the electric field (path in bold line in the inset of Fig. 3), hence doubling the production of np atoms. One therefore expects a signal of np atoms of about 5% of the initial $48s$ Rydberg atoms, which agrees reasonably well with the experimental data (see Fig. 3).

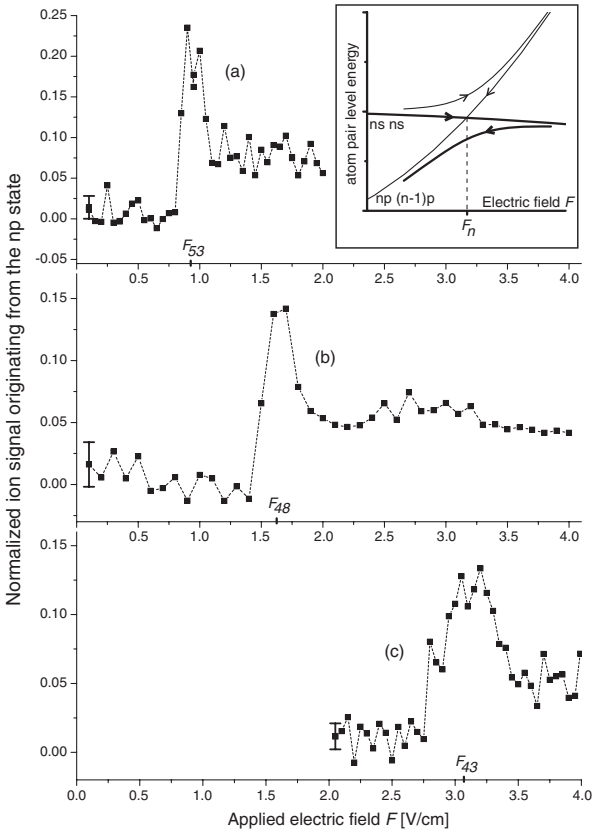

FIG. 3. Normalized ion signal resulting from the np state, after excitation to the ns state, as a function of the strength of the time-dependent applied electric field, (a) $n = 53$, (b) $n = 48$, (c) $n = 43$. The inset shows the two mechanisms for the production of $np + (n-1)p$ atom pairs (see text).

In a second series of measurements, we varied the rise time of the electric field which we apply after excitation of the sodium atoms to the $48s$ state. We set the strength of this electric field to 2.3 V/cm, i.e., 0.5 V/cm greater than F_{48}. All other parameters remain as above. In the left panel of Fig. 4 is shown the measured dependence of the normalized ion signal originating from the $48p$ state, as a function of the rise time τ of the applied electric field. As can be seen above, r_0 scales as $(dF/dt)^{-1/6}$ hence as $\tau^{1/6}$. The fraction of atoms having their nearest neighbor at less than r_0 scales as r_0^3, leading to a production of $48p$ Rydberg atoms through adiabatic transitions scaling as $\tau^{1/2}$. This law is very well reproduced experimentally, as

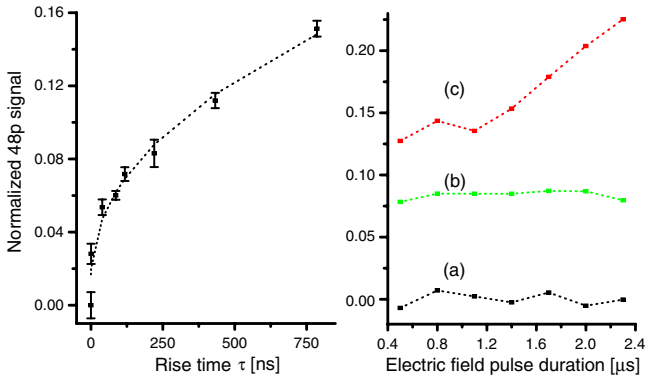

FIG. 4 (color online). Left: normalized ion signal resulting from the $48p$ Rydberg atoms, as a function of the rising time τ of the applied electric field. Dashed line: adjustment of the $\tau^{1/2}$ law to the experimental data, which accounts for the LZ adiabatic transitions (see text). Right: normalized ion signal resulting from the $48p$ Rydberg atoms, as a function of the duration of the applied electric field, for various strengths of this field, (a) $F < F_{48}$: no transfer, (b) $F > F_{48}$: LZ transfer, (c) $F \simeq F_{48}$: resonant collisions.

illustrated by the least-squares fit to the experimental data shown in the left panel of Fig. 4 (dashed line).

Moreover, we have investigated the production of $48p$ atoms as a function of the time the Rydberg atoms spend in the applied electric field. To do so, we set the rising time of the applied electric field to 220 ns again and we vary the duration of the pulse. The right panel of Fig. 4 shows the dependence of the normalized ion signal originating from the $48p$ atoms, as a function of the duration of the applied field for three values of the field strength. If the electric field F does not exceed F_{48} [curve (a): 1.1 V/cm], the $48p$ atoms are solely produced by blackbody-induced transitions. If the field allows resonant collisions [$F \simeq F_{48}$, curve (c): 1.8 V/cm] the additional $48p$ atom signal varies linearly with the time the atoms spend at this field. However, if the applied electric field is greater than F_{48} [curve (b): 2.3 V/cm], a constant additional amount of $48p$ atoms is observed, independently of the time duration the atoms experience the applied electric field. This rules out nonresonant collisions between 48 s atoms, and confirms that only the way the electric field varies with time and crosses F_n matters for the production of pairs of $np + (n-1)p$ atoms.

To conclude, we have presented the experimental evidence for adiabatic Landau-Zener transitions in pairs of Rydberg atoms in a supersonic beam, induced by varying in time a homogeneous electric field. We control the efficiency of the process by tuning the sweeping rate of the electric field. In the context of deceleration of Rydberg atoms or molecules [18,19], the changes of the internal state of Rydberg particles, induced by changes of the state of pairs experiencing a changing electric field, might reduce the efficiency of deceleration and trapping of Rydberg species. As the final pair state detected in our experiment is by nature an entangled state, due to the indistinguishability of both atoms, we expect this work to lead to a new, convenient method to entangle atoms in a controlled manner.

This work has been mainly financed by an ANR grant (NT05-2 41884) and by the "Institut Francilien de Recherche sur les Atomes Froids" (IFRAF). J. B. acknowledges support from the aforementioned ANR grant. The authors thank F. Merkt for enlightening discussions.

*Present address: Laboratoire Kastler Brossel, Ecole Normale Supérieure, 24 rue Lhomond, 75231 Paris Cedex 05, France.
†Corresponding author.
nicolas.vanhaecke@u-psud.fr

[1] T. F. Gallagher and P. Pillet, *Advances In Atomic, Molecular, and Optical Physics* (Academic Press, 2008), Vol. 56, pp. 161–218.
[2] K. A. Safinya, J. F. Delpech, F. Gounand, W. Sandner, and T. F. Gallagher, Phys. Rev. Lett. **47**, 405 (1981).
[3] M. J. Renn and T. F. Gallagher, Phys. Rev. Lett. **67**, 2287 (1991).
[4] W. R. Anderson, J. R. Veale, and T. F. Gallagher, Phys. Rev. Lett. **80**, 249 (1998).
[5] I. Mourachko, D. Comparat, F. de Tomasi, A. Fioretti, P. Nosbaum, V. M. Akulin, and P. Pillet, Phys. Rev. Lett. **80**, 253 (1998).
[6] A. Fioretti, D. Comparat, C. Drag, T. F. Gallagher, and P. Pillet, Phys. Rev. Lett. **82**, 1839 (1999).
[7] D. Jaksch, J. I. Cirac, P. Zoller, S. L. Rolston, R. Côté, and M. D. Lukin, Phys. Rev. Lett. **85**, 2208 (2000).
[8] M. D. Lukin, M. Fleischhauer, R. Cote, L. M. Duan, D. Jaksch, J. I. Cirac, and P. Zoller, Phys. Rev. Lett. **87**, 037901 (2001).
[9] T. Vogt, M. Viteau, J. Zhao, A. Chotia, D. Comparat, and P. Pillet, Phys. Rev. Lett. **97**, 083003 (2006).
[10] R. Heidemann, U. Raitzsch, V. Bendkowsky, B. Butscher, R. Löw, and T. Pfau, Phys. Rev. Lett. **100**, 033601 (2008).
[11] A. Gaetan, Y. Miroshnychenko, T. Wilk, A. Chotia, M. Viteau, D. Comparat, P. Pillet, A. Browaeys, and P. Grangier, Nature Phys. **5**, 115 (2009), ISSN .
[12] E. Urban, T. A. Johnson, T. Henage, L. Isenhower, D. D. Yavuz, T. G. Walker, and M. Saffman, Nature Phys. **5**, 110 (2009), ISSN .
[13] J. R. Rubbmark, M. M. Kash, M. G. Littman, and D. Kleppner, Phys. Rev. A **23**, 3107 (1981).
[14] J. Han and T. F. Gallagher, Phys. Rev. A **77**, 015404 (2008).
[15] T. F. Gallagher, *Rydberg Atoms*, Cambridge Monographs on Atomic, Molecular and Chemical Physics (Cambridge University Press, Cambridge, 1994).
[16] L. Landau, Phys. Z. Sowjetunion **2**, 46 (1932).
[17] C. Zener, Proc. R. Soc. A **137**, 696 (1932).
[18] E. Vliegen, S. D. Hogan, H. Schmutz, and F. Merkt, Phys. Rev. A **76**, 023405 (2007).
[19] N. Vanhaecke, D. Comparat, and P. Pillet, J. Phys. B **38**, S409 (2005).